Planta (2006) 223: 271–282
DOI 10.1007/s00425-005-0090-2

ORIGINAL PAPER

**Thaddée Boudjeko · Christine Andème-Onzighi
Maïté Vicré · Alain-Pierre Balangé
Denis Omokolo Ndoumou · Azeddine Driouich**

Loss of pectin is an early event during infection of cocoyam roots by *Pythium myriotylum*

Received: 27 May 2005 / Accepted: 11 July 2005 / Published online: 14 September 2005

Abstract Cocoyam (*Xanthosoma sagittifolium*) is an important tuber crop in most tropical zones of Africa and America. In Cameroon, its cultivation is hampered by a soil-borne fungus *Pythium myriotylum* which is responsible for root rot disease. The mechanism of root colonisation by the fungus has yet to be elucidated. In this study, using microscopical and immunocytochemical methods, we provide a new evidence regarding the mode of action of the fungus and we describe the reaction of the plant to the early stages of fungal invasion. We show that the fungal attack begins with the colonisation of the peripheral and epidermal cells of the root apex. These cells are rapidly lost upon infection, while cortical and stele cells are not. Labelling with the cationic gold, which binds to negatively charged wall polymers such as pectins, is absent in cortical cells and in the interfacial zone of the infected roots while it is abundant in the cell walls of stele cells. A similar pattern of labelling is also found when using the anti-pectin monoclonal antibody JIM5, but not with anti-xyloglucan antibodies. This suggests that early during infection, the fungus causes a significant loss of pectin probably via degradation by hydrolytic enzymes that diffuse and act away from the site of attack. Additional support for pectin loss is the demonstration, via sugar analysis, that a significant decrease in galacturonic acid content occurred in infected root cell walls. In addition, we demonstrate that one of the early reactions of *X. sagittifolium* to the fungal invasion is the formation of wall appositions that are rich in callose and cellulose.

Keywords Cell wall · Cocoyam · Immunocytochemistry · Pectin · Root · Rot disease

Abbreviations PBS: Phosphate-Buffered Saline · CBH-I gold: Cellobiohydrolase colloidal gold · CMC: Carboxymethylcellulose · GalA: Galacturonic Acid · HG: Homogalacturonans · PATAG: Periodic acid-thiosemicarbazide-silver proteinate · RT: Room temperature · TEM: Transmission electron microscopy · UA: Uronic acid

T. Boudjeko · C. Andème-Onzighi · M. Vicré · A.-P. Balangé
A. Driouich (✉)
UMR CNRS 6037, IFRMP 23. Centre Commun
de Microscopie Electronique, Université de Rouen,
76821 Mont Saint Aignan, France
E-mail: Azeddine.Driouich@univ-rouen.fr
Tel.: +33-2-35146535
Fax: +33-2-35146615

D. O. Ndoumou
Department of Biology, Higher Teacher's Training College,
University of Yaoundé 1, Yaoundé, Cameroon

T. Boudjeko
Department of Biochemistry, Faculty of Science,
University of Yaoundé 1, Yaoundé, Cameroon

Introduction

Xanthosoma sagittifolium (L) Schott is an important staple food in the Gulf of Guinea, in East Africa and in Central and South America. It is called cocoyam in Cameroon and yautia or tuquisque in Central and South America. Cocoyam is a landrace cultivar consisting of three varieties (white, pink or red and yellow). Cocoyam root rot is caused by a soil-borne fungus *Pythium myriotylum* and is the most prevalent plant disease in Cameroon. The roots of infected plants are impaired in their ability to absorb mineral nutrients from the soil which results in stunted growth and leaf yellowing (Pacumbaba et al. 1992). Reduction in crop yields as high as 90% has been reported in some infected plantations in Cameroon (Schaffer 1999). Attempts to obtain productive and resistant varieties by classical methods have been hampered by genetic incompatibility between the cultivars and by the poor genetic knowledge of the available genotypes.

In the past few years, ultrastructural and cytological studies have contributed significant insight into the interaction of various host plants with pathogens such as viruses (Channarayappa et al. 1991), nematodes (Hussey et al. 1992; Valette et al. 1997, 1998), bacteria (Boyer

et al. 1997) and fungi (Daayf et al. 1997; Cambion et al. 1998; Yeddidia et al. 1999; Mims et al. 2000). Ultrastructural and cytochemical approaches have the potential to significantly improve our knowledge of how plant disease resistance is expressed at the cellular level and on the molecular mechanisms by which plants defend themselves against a variety of plant pathogens. For example, in cavity spot, one of the most virulent diseases of carrot, Cambion et al. (1998) used ultrastructural analyses to show that *P. violae* was responsible for the degradation of highly methylesterified pectins located near the hyphae, whereas *P. ultimum* was responsible for more extensive degradation of pectins and cellulose in tissues located far from the hyphae. Partially resistant cotton attacked by *Verticillium dahliae* induced ultrastructural modifications of parenchyma cells of the vascular tissues as well as a high production of terpenoids and phenolics in the host tissue (Daayf et al. 1997). Valette et al. (1998) showed that in susceptible and partially resistant cultivars of banana, infection by the nematode *Radopholus similis* was characterised by severe host cell wall alterations. This phenomenon was attenuated in the resistant cultivars by the deposition of phenolics. The hypersensitive response of *Solanum tuberosum* to *Phytophthora infestans* differs considerably between clones and is correlated to deposition of callose and extracellular globules containing phenolic compounds (Viviane et al. 2000). In symbiotic associations between plants and fungi, the penetration of the fungus is generally restricted to the epidermis and the outer cortex. In this case, the colonisation of the plant tissue is characterised by strengthening of the cell walls through wall apposition containing large amounts of callose and infiltrations of cellulose (Yeddidia et al. 1999). In the hemibiotrophic interaction between *Photinia fraseri* and *Entomosporium mespili*, the fungus produces distinctive haustoria that terminate in the living cells of young lesions. In older lesions, the haustoria terminate in hyphae that grow indiscriminately between and through dying and dead host cells (Mims et al. 2000).

In spite of its importance in African and American agriculture, no research has been undertaken on the mode of colonisation of *X. sagittifolium* roots by *P. myriotylum* or on the reaction of the plant to the invading agent. Information on possible morphological changes the fungus undergoes in host cells, the manner of penetration of the fungus and alterations that may occur in the host cell in response to the infection is essential for a meaningful interpretation of fungus/host cell interaction. Thus, we performed a study of ultrastructural, cytochemical and biochemical changes that occurred in *X. sagittifolium* roots infected by *P. myriotylum*. Our aim was to trace the path of the penetration of the mycelium in the root tissue and characterise the host cell wall alterations induced by the pathogen. To the best of our knowledge, the results obtained represent the first report on cell wall alterations of *X. sagittifolium* roots infected by the fungus *P. myriotylum*.

Materials and methods

Six-week-old tissue culture-derived cocoyam plantlets [*Xanthosoma sagittifolium* (L) Schoot, white cultivar] were obtained by shoot multiplication at the Laboratory of Plant Physiology, Higher Teacher's Training College, University of Yaoundé I. Cameroon (see Omokolo et al. 1995). This procedure was necessary for the production of a uniform population of plantlets.

Pythium myriotylum isolates were obtained from diseased cocoyam roots harvested from the Yaoundé region (Cameroon) and purified according to Xu et al. (1995). Four-day-old fungal cultures were used as inoculums.

Plant inoculation

Plantlets were inoculated following the procedure of Tambong et al. (1999) with minor modifications. Briefly, cocoyam plantlets were removed aseptically from the culture tubes, rinsed with sterilised distilled water and inoculated in test tubes containing 20 ml of Murashige and Skoog (1962) mineral salt medium and one mycelial agar plug (0.4 cm in diameter). Test tubes were then incubated at 28°C for 48 h (culture cabinet, P Selecta Hotgold-GL). Test tubes inoculated with mycelium-free agar plugs were used as control.

Sample preparation for transmission electron microscopy (TEM)

Root apices (1–2 mm) were excised and fixed as described previously (Vicré et al. 1998) with minor modifications. Briefly, the samples were incubated for 2 h in a 4% glutaraldehyde solution in 0.1 *M* cacodylate buffer pH 7.2, washed twice and immersed for 15 min in the same buffer. After a post-fixation for 1 h in a 1% (w/v) osmium tetroxyde solution followed by thorough rinsing, the root tips were dehydrated in a graded ethanol series. Samples were then embedded in London Resin White, (Oxford Agar, Oxford, UK) by serial immersion in graded resin–alcohol mixtures (30 min each in 25%, 50% and 75%, v/v) and then in pure resin for 24 h at room temperature (RT). Polymerisation was carried out overnight at 60°C. Thin (1 μm) and ultra thin (90 nm) sections were obtained with an ultramicrotome (Reichert ultracut, E) collected on multi-well glass slides for light microscopy or gold grids (300 mesh, Oxford Agar) for TEM.

Immunofluorescence microscopy

Fresh healthy and infected young roots were fixed for 1 h at RT in 50 *mM* Pipes buffer containing 4% (w/v) paraformaldehyde, 1% (v/v) glutaraldehyde and 1 *mM* $CaCl_2$, pH 7.2. Following fixation, the roots were washed twice with 50 *mM* Pipes, 1 *mM* $CaCl_2$, pH 7.2 and then three to four times with 0.01 *M* phosphate-buffered

saline (PBS: prepared from a 10× stock solution containing 80 g NaCl, 2.01 g KCl, 2.04 g KH_2PO_4 and 9.93 g Na_2HPO_4, $12H_2O$ in 1 l dH_2O, pH 7.2) for 10 min each. After washing, immunofluorescence labelling was performed as described previously (Andème-Onzighi et al. 2002). Fresh intact root apices were collected and incubated in 0.01 *M* PBS pH 7.2, containing 3% (w/v) non-fat-dried milk (PBS–milk = blocking solution) for 30 min, and then placed for 2 h at RT in tenfold dilution of JIM5 and anti-XG antibodies and 100-fold dilution for anti-β-1,3-glucans antibody. Samples were washed in PBS and then incubated with 100-fold dilution of appropriate secondary antibodies, anti-rat IgG, anti-rabbit IgG or anti-mouse IgG (whole molecule) conjugated to fluorescein isothiocyanate (FITC; Sigma) in PBS–milk for 2 h in darkness at RT. The samples were thoroughly washed in PBS and mounted in a glycerol-based anti-fade solution (Citifluor^{TM} AF1, Agar Scientific, UK) and then observed on an LEICA-DMLB microscope equipped with epifluorescence coupled with LEICA DFC 300FX camera. Controls were performed by omitting either the primary antibody or by its pre-absorption with laminarin (Biosupplies Parkville, Australia).

Toluidine blue staining

Thin sections were stained (3–5 min) with toluidine blue (0.5% w/v in 2.5% w/v Na_2CO_3) at 55–60°C on hot plate, rinsed with distilled water and air-dried before observation with a Zeiss microscope (Axioscope MC-100).

Periodic acid-thiosemicarbazide-silver proteinate test (PATAg Test) for the detection of polysaccharides

Ultrathin cross sections were stained with PATAg test following the procedure of Thiéry (1967). The sections were then floated on a 1% (w/v) periodic acid solution for 30 min and rinsed twice for 10 min each in distilled water. They were maintained for 45 min on a 0.2% (w/v) thiosemicarbazide solution in 20% (v/v) acetic acid, washed in solutions of progressively decreasing acetic acid concentration and finally in pure water. The sections were treated with 1% (w/v) silver proteinate for 30 min in the dark. Grids were thoroughly rinsed and air-dried before observation with a Phillips Tecnai 12 TEM (at CCME, University of Rouen) operating at 80 KV. Grids floated on distilled water instead of periodic acid solution were used as controls.

Labelling with cationic colloidal gold complex for the detection of polysaccharides and protein anionic sites

Labelling of anionic sites was performed as a one-step procedure according to Skutelsky and Roth (1986). Ultrathin sections were incubated in 3% acetic acid pH 2.6 for 15 min. The sections were treated with 10-nm cationic colloidal gold complex diluted 1/100 (v/v) in 3% acetic acid for 1 h at room temperature. The samples were then rinsed thoroughly with 3% acetic acid and finally with distilled water. They were stained with PATAg as described in His et al. (2001). The control experiments were performed as follows: (i) enzymatic treatment of the samples in a proteinase K (proteinase type IX from *Tritirachium album*) solution (1 mg/ml proteinase K in 0.05 *M* Tris–HCl buffer pH 8.0) at room temperature for 1 h (Vreeland et al. 1989); (ii) chemical methyl esterification in 1/5 (v/v) acetyl chloride/absolute methanol at 4°C for 72 h; (iii) combination of control 1 and control 2; (iv) pre-incubation of the cationic gold complex for 1 h with polygalacturonic acid at 1 mg/ml in 3% acetic acid before labelling.

Immunogold labelling of pectin, xyloglucan and callose

Immunogold labelling of pectins was performed using the rat monoclonal antibody JIM5 specific for homogalacturonans (HG; Knox et al. 1990; Willats et al. 2000). Ultrathin cross sections were floated on a blocking solution: 0.01 *M* phosphate buffer saline (PBS) pH 7.4, containing 3% (w/v) non-fat-dried milk and 1% (v/v) Tween 20 (PBST) for 30 min. The grids were blotted dry and then placed in a drop of primary antibody and incubated at 4°C overnight. After washing in a continuous stream of PBST, the secondary antibody conjugated to 20-nm gold (goat anti-rat IgG) diluted 1/25 in buffer was applied for 1 h at RT. The grids were rinsed for 30 min with PBST followed by distilled water and then stained with PATAg. Xyloglucan labelling was performed using anti-XG antibodies as described previously (Zhang et al. 1996).

The monoclonal antibody specific for β-1,3-glucans (Biosupplies) was used for immunolocalisation of callose. Sections were incubated for 30 min at RT on the blocking solution, then incubated for 4 h at RT in a drop of the primary antibody diluted 1/25 in the PBST buffer before being incubated with the secondary goat anti-mouse antibodies (1/25) conjugated to colloidal gold (20 nm). Controls were performed by the omission of the primary antibody incubation step.

Enzyme–gold affinity for cellulose labelling

Labelling of β-1,4-glucans was performed using a cellobiohydrolase colloidal gold complex (CBH I-gold complex) prepared according to Bonfante-Fasolo et al. (1990). Ultrathin sections were floated on 0.05 *M* citrate phosphate buffer (CPB) pH 4.5 for 10 min, and treated for 30 min with a 1/100 enzyme–gold stock solution diluted in CPB. The grids were then floated on the incubation buffer alone for 5 min, rinsed twice with CPB and air-dried. Finally, the sections were post-stained

with PATAg. Control sections were treated with an enzyme–gold complex solution to which carboxymethylcellulose (CMC) had been added at 1 mg/ml 1 h before use (Berg et al. 1988).

Cell wall preparation and uronic acid (UA) content determination

Cell walls from healthy and infected root apices were extracted and monosaccharide composition determined as described previously (Ray et al. 2004). For pectin extraction, cell walls were extracted twice with 5% ammonium oxalate at 100°C with constant stirring. After centrifugation at $6000 \times g$, supernatants were pooled, filtered, dialysed against water (milliQ) for 24 h, lyophilised and weighed. Total UA content of cell wall extract and oxalate fractions was estimated according to the method of Bluemenkrantz and Absoe-Hansen (1973). UA content was expressed in mg (equivalent of galacturonic acid) per mg of cell wall or oxalate fraction. Statistical analyses were performed by ANOVA using Turkey–HSD multiple range tests of the "SPSS statistical package, release 11.0" for Windows.

Results

Structural changes of host root cells

Two days after infection of cocoyam tissue culture-derived seedlings by *P. myriotylum*, the destruction of the host external tissue was observable in the epidermis and the outer cortex cells (Fig. 1). The root cap was almost completely lost in most roots examined. At 2 days, the fungal colonisation was limited to the external cell layers of the cortical parenchyma (Fig. 1b, d). The fungal mycelium was easily discernable due to the intense staining of the cytoplasm with toluidine blue (Fig. 1d). Electron microscopic examination showed that the fungus was present in the cytoplasm of host cells and in the intercellular space (Fig. 2). Numerous dense compounds, which were very reactive to PATAg, accumulated within the vacuoles of host cells (Fig. 2b) and some dissolution of the cell wall was observed in the regions surrounding the hyphae (Fig. 2e). Wall appositions produced by host cells were generally found to occur at the point of contact with the fungus (Fig. 2c).

In order to investigate the possible alterations of cell wall components in infected tissues, immunofluores-

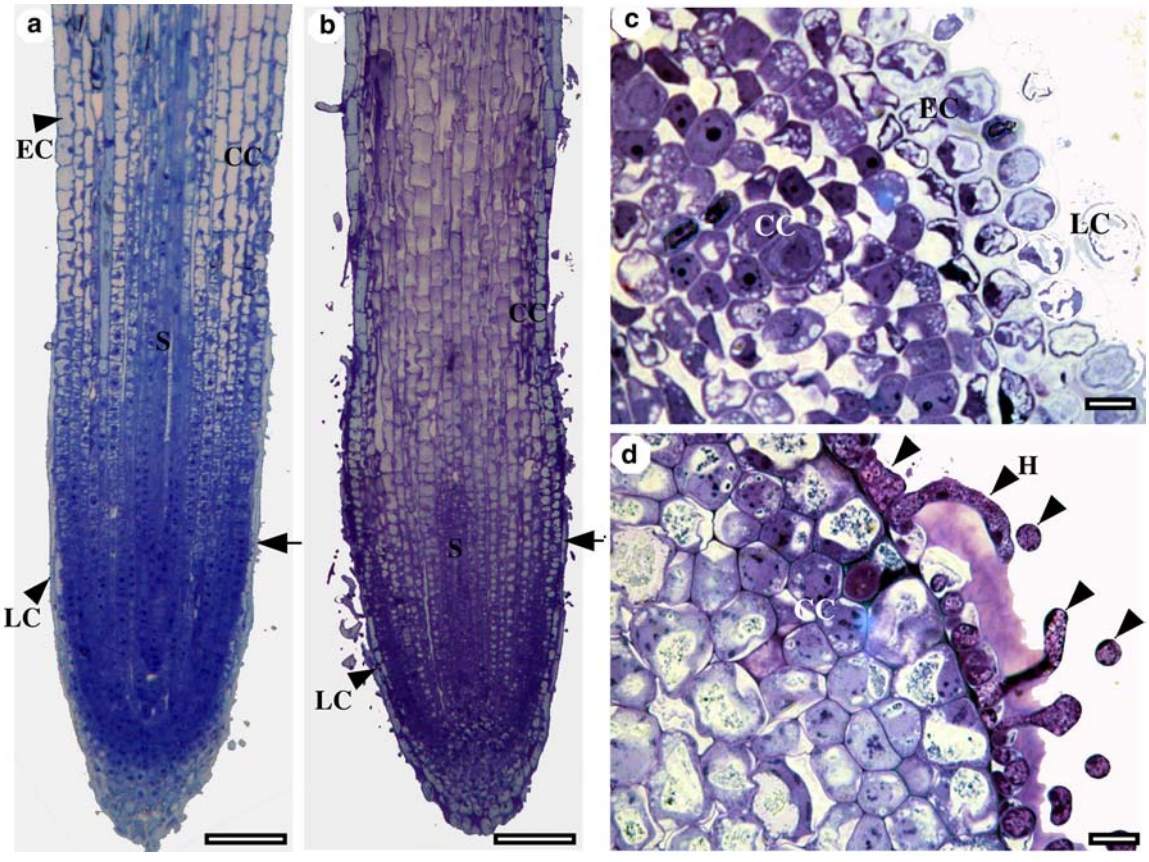

Fig. 1 (**a–d**) Toluidine blue staining of *Xanthosoma sagittifolium* root colonisation by *Pythium myriotylum* . **a** and **c** Light micrographs of longitudinal and transverse sections of healthy roots showing lateral root cap cells (LC) epidermal cells (EC), cortical cells (CC) and the stele (S). **b** and **d** Light micrographs of longitudinal and transverse sections of infected roots showing the same tissues as above. Note rotting of lateral and epidermal cell layers. H, Hyphae. The *arrows* indicate where the transverse sections were made and *arrowheads* in **d** point to the hyphae. *Scale bars*: 420 μm (**a**,**b**); 0.2 μm (**c**, **d**)

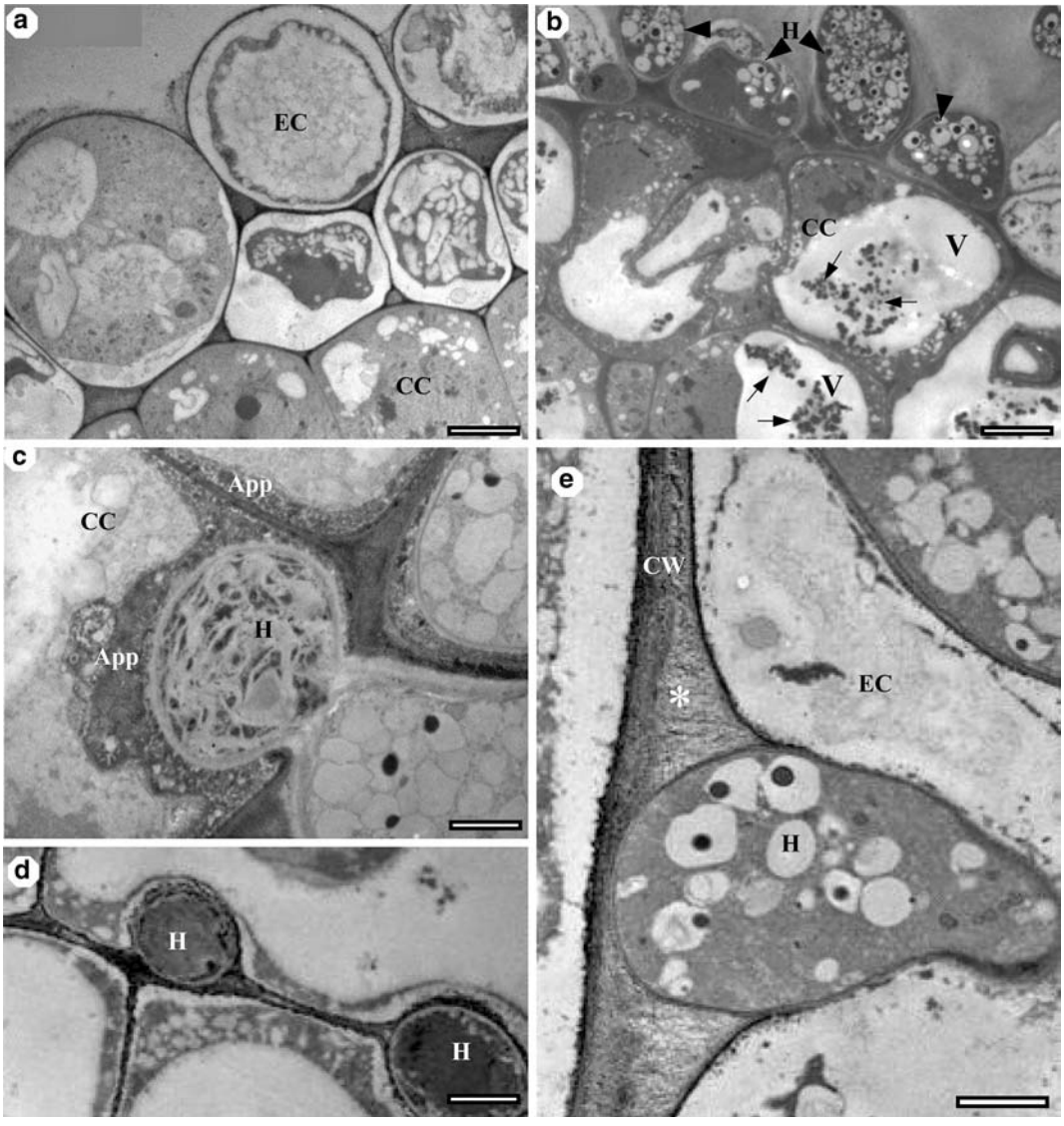

Fig. 2 (*a–e*) Transmission electron micrographs of healthy and infected root cells stained with periodic acid-thiosemicarbazide-silver proteinate (PATAg). **a** Normally looking cells of the cortex in healthy roots. **b–e** Root cells from infected plants showing the location of hyphae (H, *arrowheads*) and damages caused by the fungus. Note the presence of the fungus in between two host cells (**d**) or penetrating the cytoplasm (**e**). Some dissolution of the cell wall is also observed (* in **e**). Note the accumulation of electron dense compounds in the vacuole (V, *arrows* in **b**) and wall appositions (App) in **c**. CC, cortical cells; CW, cell wall; EC, epidermal cells. *Scale Bars*: 4 μm (**a**); 3 μm (**b**); 1 μm (**c**); 2 μm (**d**); 1.5 μm (**e**)

cence staining with three antibodies (i.e. JIM5, anti-XG and anti-callose) was performed on fresh healthy and infected root apices. As shown in Fig. 3b, JIM5 stained weakly or didn't infect roots at all. The anti-callose antibody did not stain healthy roots, whereas it strongly stained the tips of infected roots (Fig. 3d). In contrast, anti-XG did not show any major changes in staining between healthy and infected roots (Fig. 3e, f). These observations suggest that the fungus causes pectin and callose alterations in root cell walls. Therefore, we expanded upon these observations using immunogold labelling and transmission electron microscopy.

Loss of acidic pectins from cell walls upon infection

As PATAg staining and immunofluorescence light microscopy revealed wall alteration upon fungal infection (Fig. 2), we next investigated the host cell wall polymers which were likely to be affected by the fungus. Thus, cytochemical observations were conducted on the interfacial zone between the host cell and the fungus, on the cell wall of the cortical parenchyma cells (cells adjacent to infected ones) and on the cell wall of cells of the central cylinder (stele cells), following labelling with various probes.

As shown in Fig. 4, labelling with the cationic gold, which binds to the negatively charged groups of wall polymers such as pectins, revealed that in healthy roots, the gold particles were present in the cell walls of all root tissues. In infected roots, there was no labelling of the

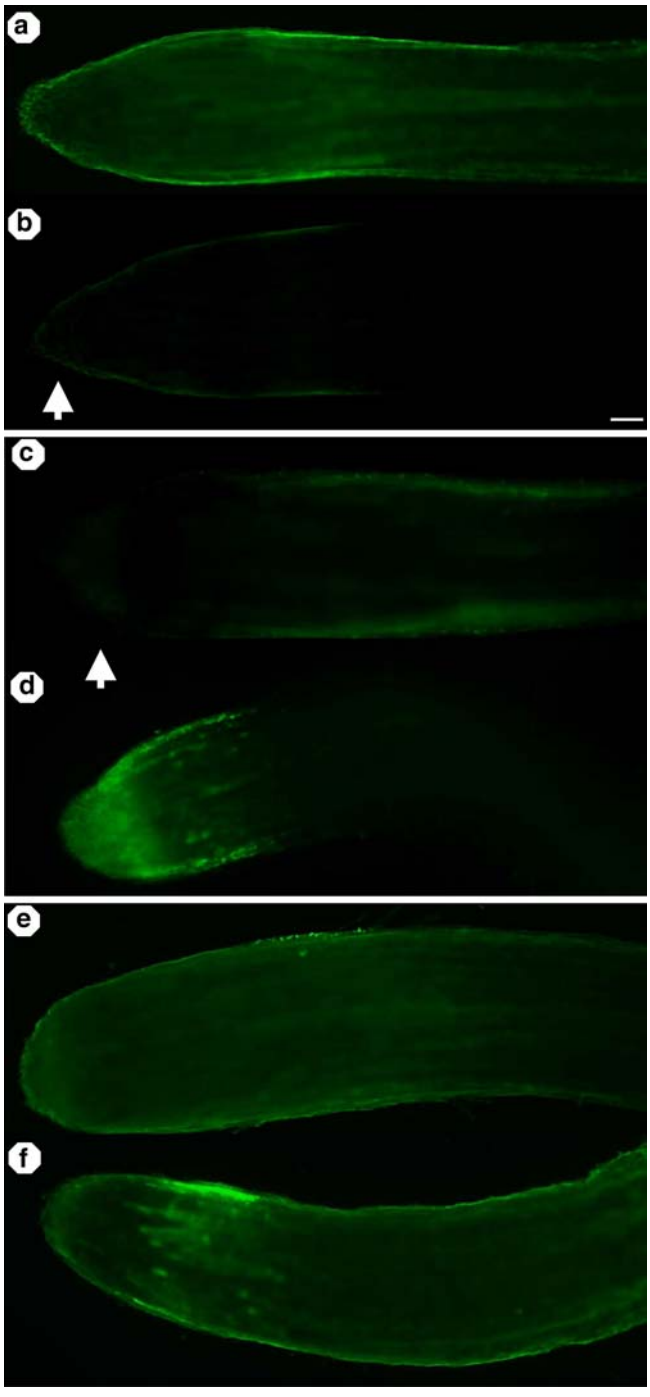

Fig. 3 (**a**–**f**) Immunofluorescence staining of pectins with the mAb JIM5 (**a**, **b**), callose with the anti-β-1,3-glucan monoclonal antibody (**c**, **d**) and xyloglucan with anti-XG antibodies (**e**, **f**) on intact fresh healthy (**a**, **c**, **e**) or infected (**b**, **d**, **f**) cocoyam roots. *Arrows* indicate root tip. *Scale bar* (same for all): 100 μm

walls of the interfacial zone or the walls of cortical cells (Fig. 4b, d), while gold particles were observed in the walls of stele cells (Fig. 4f). In control experiments, labelling of root tissues with the cationic gold probe, after pre-incubation with polygalacturonic acid, was completely abolished (data not shown). Similarly, when sections were pre-treated with acetyl chloride/methanol to chemically methylesterify the anionic groups, no labelling of the walls were observed. This indicates that, in our conditions, acidic pectins were the main wall components recognised by the cationic gold probe and that these polysaccharides were most probably lost from cortical tissues upon infection.

To further extend on this observation, we labelled root tissues of both healthy and infected plants with the mAb JIM5, which is specific for homogalacturonans (Willats et al. 2000). In infected plants, we consistently found very weak or no labelling of the interfacial zone or across the walls of the cortex cells (Fig. 5b, d). In contrast, in the walls of cells in the stele, JIM5 labelling was localised in the middle lamella and in the intercellular junctions (Fig. 5f). In healthy cocoyam roots, all the tissues were labelled (Fig. 5a, c, e). These data support the observations made with cationic gold probe (see Fig. 4).

Decrease of galacturonic acid (GalA) content of cell walls of infected tissues

To further investigate the effect of the infection on pectins, we first isolated cell walls and a pectin-rich fraction from healthy and infected root apices and determined UA content. As shown in Table 1, the yield of cell wall material and the oxalate-pectic containing fraction isolated from infected root apices was much lower than that of healthy ones. Similarly, total UA content in both fractions was reduced by 37% and 44.5%, respectively, upon infection (Table 1). In addition, the monosaccharide composition of cell walls isolated from healthy and infected root tips showed that the decrease in UA content was due specifically to a decrease in GalA (Table 2). These data further support that a loss of pectin molecules (e.g. HG) occurred upon fungal attack. Interestingly, glucose content was twice as high in cell walls of infected root tips as that found in those of healthy plants (Table 2) consistent with the observation of callose accumulation in infected root tips using microscopy (see below).

Localisation of cellulose, xyloglucan and callose in infected tissues

The distribution of β-1,4-glucans was investigated using the CBH I-gold probe. Application of the CBH I-gold probe to sections of infected or healthy cocoyam roots resulted in a distribution of gold particles all over the cell walls of all tissues examined (Fig. 6a–d). β-1,4-glucans were also detected over the cell wall of the fungus (Fig. 6b). Careful examination of the sections revealed that, in infected root, labelling was more intense in the interfacial zone between the host cell wall and the fungus cell wall (Fig. 6b). Wall appositions were also strongly labelled with the probe (Fig. 6b). Control tests including pre-incubation of the CBH-1 gold complex with CMC prior to labelling of the sections resulted in a failure of

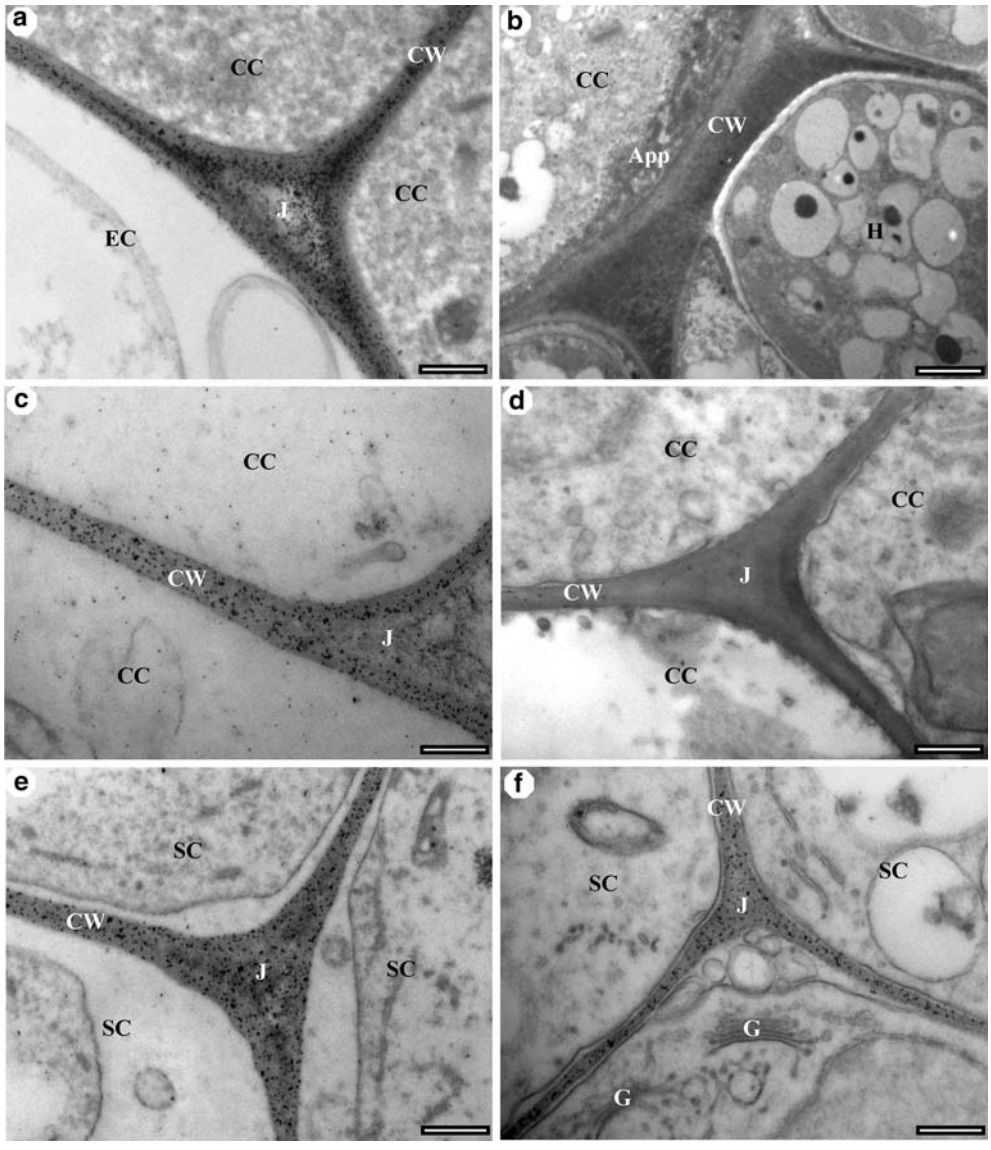

Fig. 4 (**a**–**f**) Electron micrographs illustrating labelling with the cationic gold probe in healthy (**a**, **c**, **e**) and infected (**b**, **d**, **f**) root tissues of *X. sagittifolium*. Note the absence of labelling over the cell walls of the interfacial zone and of the cortex of infected roots in **b** and **d**, and its presence in healthy roots in **a** and **c**. In **e**, **f**, positive labelling of the cell walls in stele cells of infected and healthy roots. App, wall appositions; CC, cortical cells; CW, cell wall; EC epidermal cells; G, Golgi stacks; H, hyphae; J, intercellular junction; SC, stele cells. *Scale bars*: 0.4 μm (**a**, **c**); 0.8 μm (**b**); 0.5 μm (**d**, **e**, **f**)

labelling both in the host and the fungus cell walls (not shown). Similarly, labelling with anti-XG antibodies revealed a distribution of gold particles uniformly over the cell walls of all tissues examined as illustrated in Fig. 6e, f. Xyloglucan epitopes were also localised over the cell wall of the fungus (Fig. 6g).

Labelling with the anti β-1,3-glucan monoclonal antibody revealed that in host cells a strong labelling was mainly found within wall appositions (Fig. 7b). Labelling was also found over the cell wall and in the cytoplasm of the fungus (Fig. 7b). Nearly no labelling of the cell wall was observed in healthy roots (Fig. 6a), nor in control sections when no primary antibody was used (Fig. 6c).

Discussion

The goal of this study was to investigate the early alterations of cocoyam roots infected by *P. myriotylum* in a controlled hydroponic system. Our observations showed that symptoms of root rot were evident within 48 h after infection and that, unlike xyloglucan, a marked loss of pectin substances occurred. Furthermore, our findings support the pathogenicity investigations of Pacumbaba et al. (1992) and Tambong et al. (1999) who reported that *P. myriotylum* is the unique causal agent of the cocoyam root rot disease as opposed to the claim that a complex of three root pathogens comprising *Rhizoctonia solanii* and *Fusarium solanii*, that are always associated with *P. myriotylum* in rotted roots, is needed to cause the disease (Agueguia et al. 1991).

Ultrastructural analyses of the cocoyam root/*P. myriotylum* interaction showed that fungal colonisation was associated with the host cell wall alterations. The cell wall of higher plants is a complex macromolecular structure consisting mainly of pectin, hemicellulose and cellulose polymers. It plays numerous structural, protective and growth-regulating functions in the life of the plant (Carpita and Gibeaut 1993). Given that the cell

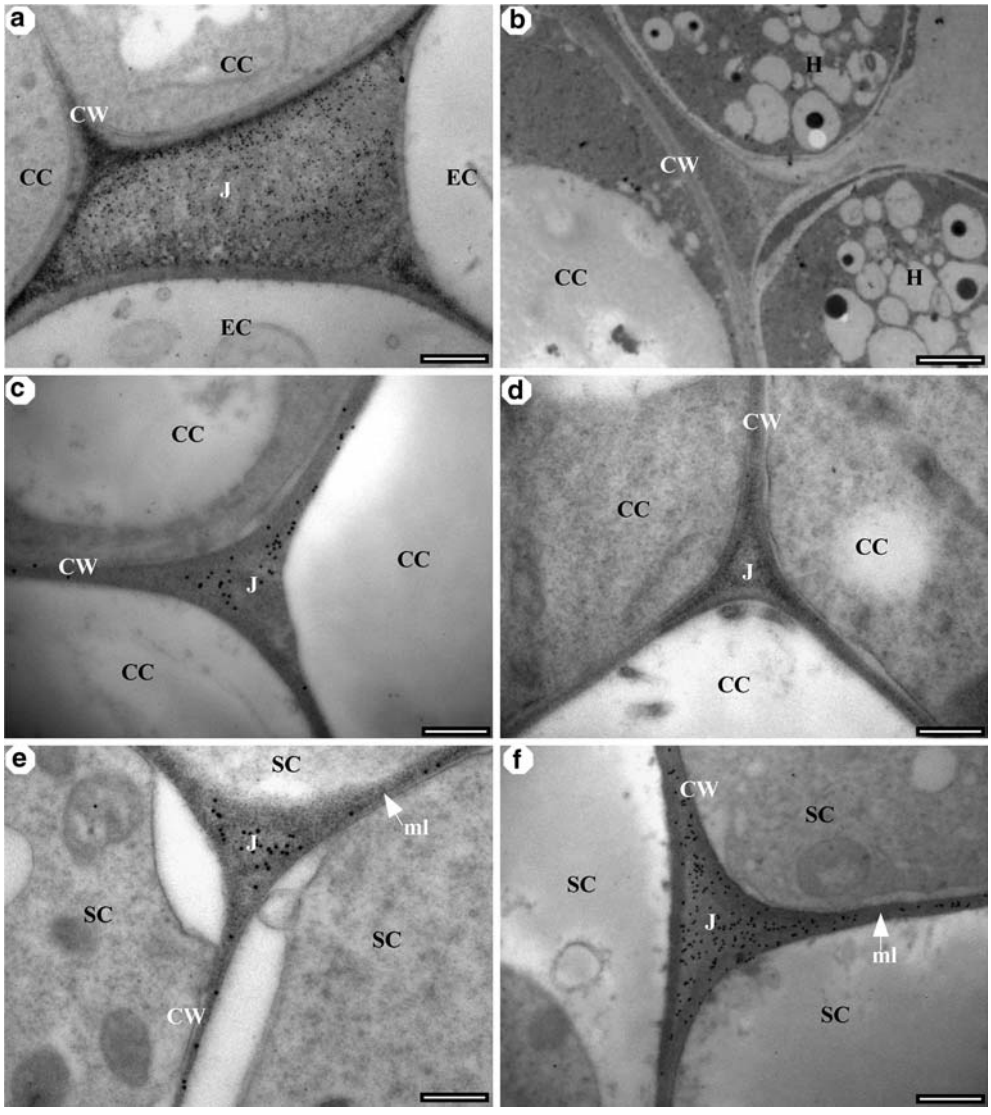

Fig. 5 (**a**–**f**) Electron micrographs showing labelling with the mAb JIM5 of the cell walls of healthy (**a**, **c**, **e**) and infected (**b**, **d**, **f**) root tissues. Note the absence of labelling in the interfacial zone and in the walls of the cortex cells in **b** and **d** but its presence in the walls of the stele cell junctions in **f** as in **e**. EC, epidermal cell; CC, cortical cells; CW, cell wall; H, hyphae; J, intercellular junction; ml, middle lamellae; SC, stele cells. *Scale bars*: 0.8 µm (**a**); 1 µm (**b**) 0.5 µm (**c**–**f**)

Table 1 Cell wall yield and uronic acid contents in healthy and infected roots of *X. sagittifolium*. Mean values ± SE ($n = 6$)

	Cell wall extracts		Oxalate fractions	
	Healthy roots	Infected roots	Healthy roots	Infected roots
Yield ($mg.g^{-1}$.Fw)	193 ± 0.01	131 ± 0.02	21 ± 0.00	10 ± 0.00
Uronic acid contents ($mg.g^{-1}$ of extract)	0.18* ± 0.01	0.10* ± 0.03	0.38 ± 0.01	0.24 ± 0.02

*Not significantly different

wall is the first line of defence against the outside environment; its disassembly is commonly observed in the rotting process caused by *Pythium* spp. (Dube and Prabakaran 1989; Zamski and Peretz 1996). Such a disassembly of plant cell wall is mediated by fungal extracellular enzymes such as pectinases and cellulases (Chen et al. 1998). In our conditions, labelling of anionic sites of acidic pectins with cationic colloidal gold complex, following plant infection, was not observed in the interfacial zone between the host cell and fungus mycelium as well as in the walls of cortical cells. This was confirmed when infected plants were subjected to a more specific probe, namely the mAb JIM5, thus supporting

Table 2 Monosaccharide composition of the cell wall isolated from healthy and infected root tips of *X. sagittifolium*. Values (mean ± SE, $n = 6$) are mol percentage of the sugar recovered. The difference between healthy and infected roots is significant at $P < 0.05$

	Healthy root	Infected root
Ara	16 ± 1.00	15 ± 0.00
Rha	5 ± 1.00	5 ± 0.01
Fuc	2 ± 0.00	2 ± 0.00
Xyl	16 ± 0.50	22 ± 1.40
GalA	19 ± 1.00	14.5 ± 0.10
GluA	1 ± 0.00	1 ± 0.01
Man	3 ± 0.50	5 ± 0.02
Gal	30 ± 2.60	21 ± 0.07
Glc	7.6 ± 0.50	14 ± 0.02

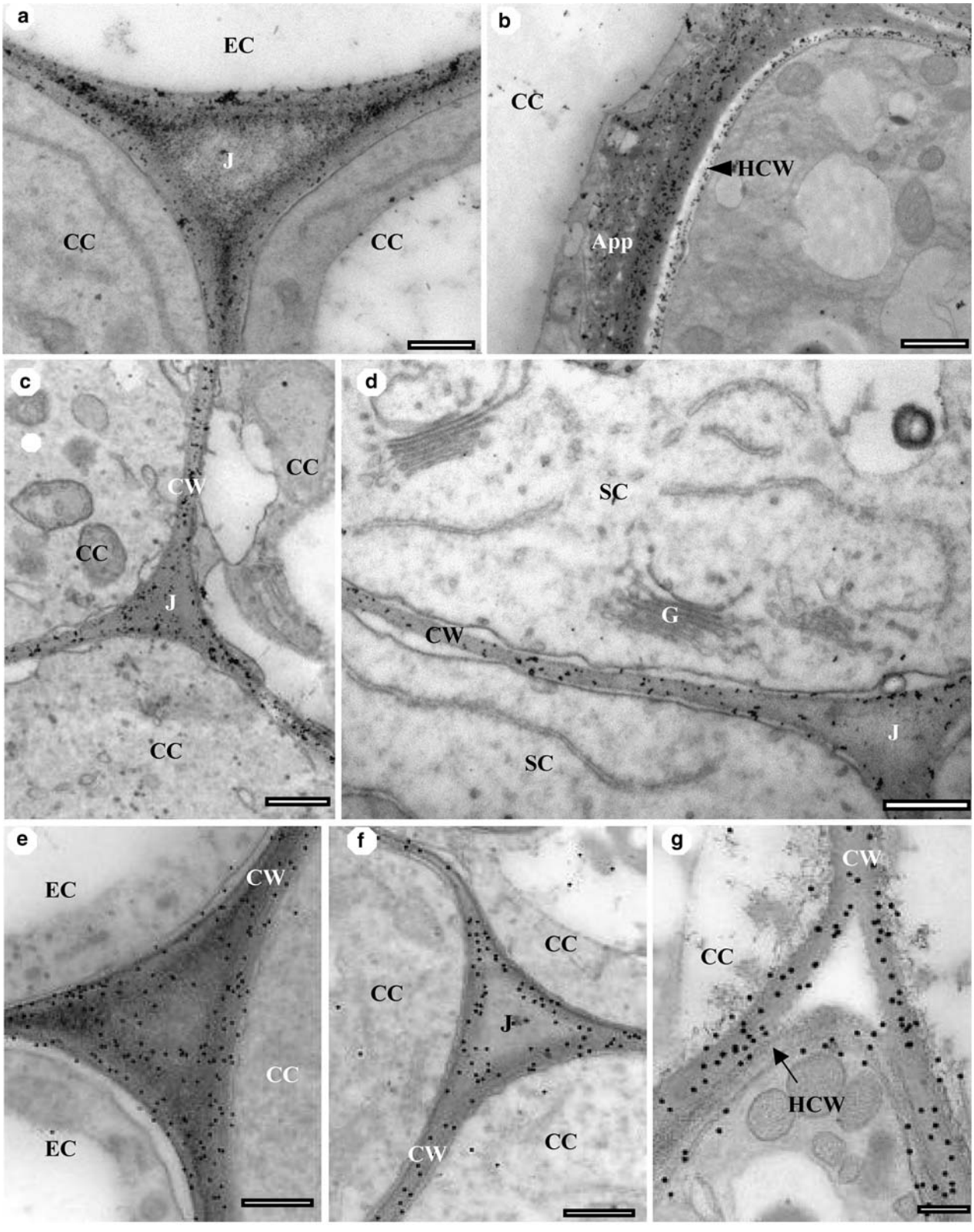

Fig. 6 (**a**–**g**) Cellulose and xyloglucan localisation. Cellulose labelling with the cellobiohydrolase-I (CBH-I) in the cell walls of healthy (**a**) and infected (**b**, **c**, **d**) root tissues. Labelling was present in the walls of the cortex, the stele and the interfacial zone. Note strong labelling of wall appositions (**b**). The walls of the hyphae were also labelled in **b**. Xyloglucan labelling with anti-XG antibodies in the cell walls of healthy (**e**) and infected (**f**, **g**) root tissues. Labelling was present in the walls of all cells. The walls of the hyphae were also labelled (**b**). App, wall appositions; CC, cortical cells, CW, cell wall; EC epidermal cells; G, Golgi stacks; H, hyphae; HCW, hyphae cell wall; J, intercellular junction; SC, stele cells. *Scale bars*: 0.33 μm (**a**); 0.5 μm (**b-f**); 0.2 μm (**g**)

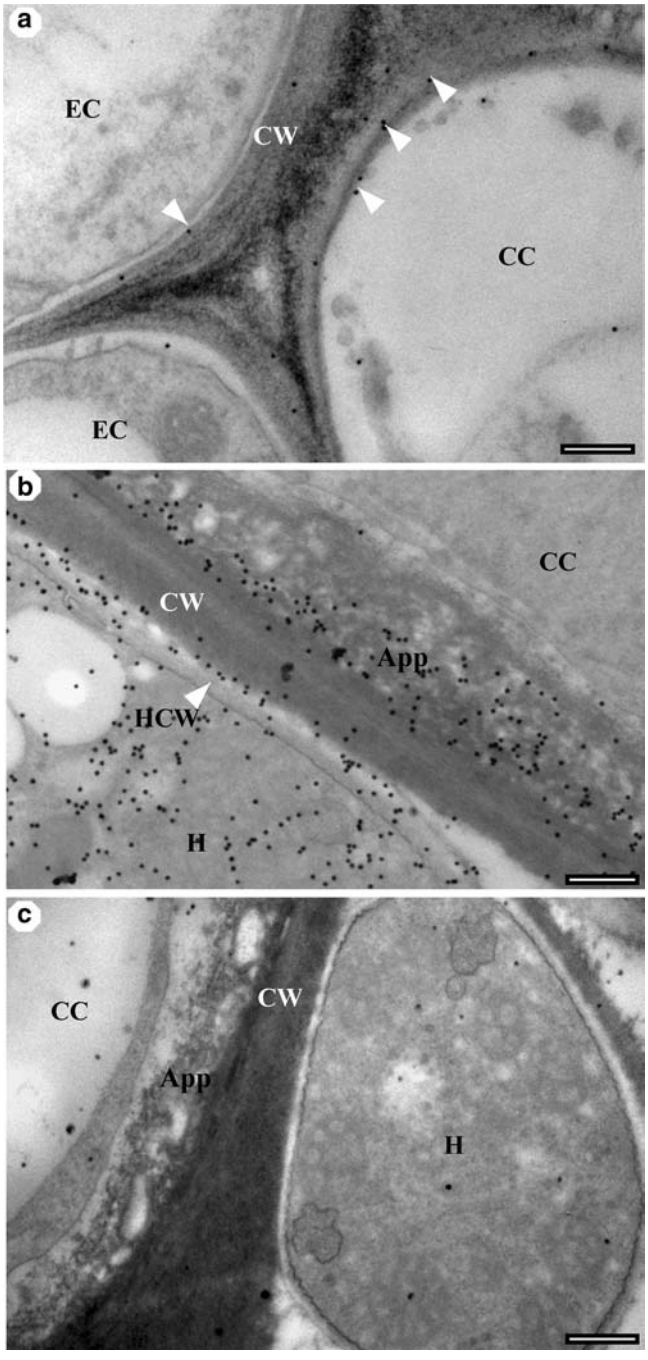

Fig. 7 (**a–c**) Immunogold localisation of callose with the anti-β-1,3-glucan antibody in the cell walls of healthy (**a**) and infected root (**b**, **c**) cells. **a** Electron micrograph illustrating labelling over the walls of cortical and epidermal cells of healthy roots. A very few gold particles are seen (*arrowheads*). **b** Electron micrograph showing strong labelling of the wall appositions, the cell wall (*arrowhead*) and cytoplasm of hyphae. **c** Control section treated without primary antibody (anti-β-1,3- glucan); note the absence of labelling. App, wall appositions; CC, cortical cells; CW, cell wall; H, hyphae; HCW, hyphae cell wall. *Scale bars*: 0.4 μm (**a**, **b**); 0.33 μm (**c**)

the fungus-induced hydrolysis of pectic HG. Pectin hydrolysis was further confirmed by a marked reduction of GalA content in infected root cell walls (see Table 2). The content of galactose, a sugar that is present in pectins such as rhamnogalacturonans and galactans, decreased, suggesting that pectins other than HG could be affected.

Our observations also showed that although hyphae were located mostly in epidermal and subepidermal cells, pectin loss extended to cortical cells that are away from the contact zone. It is likely, thus, that the fungus secretes hydrolytic enzymes that are able to diffuse and reach root cells located beyond the site of infection. This finding is consistent with results reported by Cambion et al. (1998), who showed that in carrot cavity spot, *P. ultimum* degrades pectins on sites located far from the pathogen site of attack. However, how these enzymes are transported from one site to another remains to be determined. Pectin-degrading enzymes such as pectin lyase and polygalacturonases are known to be secreted by *Pythium* species (Dube and Prabakaran 1989; Cherif et al. 1991; Chen et al. 1998) and therefore are most likely involved in pectin hydrolysis in cocoyam root cell walls observed in our conditions.

Labelling with CBH I-gold complex which is specific for cellulose (Berg et al. 1988) and with anti-xyloglucan antibodies was observed to occur uniformly over all the host cell walls (Fig. 6). However, in the case of CBH I-gold complex, labelling was more intense at the point of contact than at other zones. This may reflect an increase in cellulose deposition in specific area of host cell walls. But this could also be attributed to the accessibility of the probe to cellulose molecules resulting from partial degradation of pectins by the fungus. In a similar study performed on carrot roots infected with *P. ultimum*, Cambion et al. (1998) showed that labelling with an exoglucanase-gold probe was particularly intense over the carrot cell wall areas close to the pathogen and in wall appositions. The positive staining of the cell walls of *P. myriotylum*, which is an oomycete, with CBH I-gold complex, is in agreement with the biochemical data indicating the presence of cellulose in the cell wall of this class of fungi (Helbert et al. 1997; Werner et al. 2002).

Immunogold labelling of callose, revealed by an anti-β-1,3-glucan antibody, was also found to occur in fungal cell wall as well as in the cytoplasm. Detection of β-1,3-glucans throughout the cytoplasm of the fungus cell may be due to labelling of β-1,3-glucans of *Pythium* that are produced intracellularly and transported within secretory vesicles that originate from the Golgi-like apparatus as previously reported (Isaac 1992). This is in contrast to what is found in higher plant cells, in which callose, like cellulose, but unlike pectins, is synthesised at the plasma membrane (Driouich et al. 1993; Delmer 1999).

Callose was also extremely abundant in *Pythium*-induced wall appositions. These structures, which are commonly shown to be rich in callose and cellulose, are formed as an early plant response to infection by various pathogens (Mueller et al. 1994; Brown et al. 1998; Yeddidia et al. 1999). They are thought to play a role in strengthening the walls of host cells during fungal penetration. Nevertheless, our finding that epidermal and

cortical cells are destroyed as early as 48 h after infection and the strict localisation of callose at root apex indicates that cell wall appositions may not be an effective resistance mechanism associated with pathogenesis. Similar observations were made in roots of both susceptible and partially resistant infected banana cultivars (Valette et al. 1997). The observed callose deposition is likely to be induced by the mechanical stress resulting from host cell wall breakdown rather than being an effective barrier against pathogen ingression. In support of this, two recent studies showed that a mutant of *Arabidopsis thaliana*, in which a single glucan synthase-like gene that is essential to papillary callose synthesis, is disrupted, exhibited enhanced disease resistance to powdery mildew fungi, but not to bacterial pathogen *P. syringae* (Nishimura et al. 2003; Schulze-Lefert 2004). The fact that, cell wall appositions were localised at the root tip, where root rotting was evident, could be explained by the possible implication of callose papilla in assisting the containment of pathogen-derived elicitors or in protecting the invading fungus against plant-derived antimicrobial compounds (Gomez-Gomez and Boller 2002; Jacobs et al. 2003).

To conclude, this study presents, for the first time, the early plant reaction events that occur during infection of cocoyam roots by *P. myriotylum*. Our investigations show that *P. myriotylum* caused alterations of the host cell within 48 h. The action of the fungus begins with a rapid hydrolysis of cell wall pectins, but not xyloglucan, at the sites of contact as well as beyond the contact zone. Early responses of host cells involve the formation of wall appositions filled with callose and cellulose as well as an accumulation of densely stained phenolic-like compounds within the vacuoles. The use of labelling techniques to localise specific cell wall-degrading enzymes within cocoyam tissue infected by *P. myriotylum* would aid in the further elucidation of the mechanism by which the infection process of *P. myriotylum* operates to cause cocoyam root rot disease.

Acknowledgements The authors would like to acknowledge "Le Service des Relations Internationales de l'Université de Rouen" for financing exchange visits between France and Cameroon. Thanks are also due to Dr M.L. Follet Gueye research assistance during the stay of BT at the University de Rouen, to L. Chevalier and to Dr C. Rihouey for their excellent technical assistance. We are indebted to Dr P. Knox (University of Leeds, UK) and Pr A. Staehelin (University of Colorado, USA) for the gift of the antibodies. J. Moore (University of Cape Town, RSA) is also thanked for critical reading of the manuscript.

References

Agueguia A, Fatakun CA, Hahn SK (1991) The genetics of resistance to cocoyam root rot blight complex disease in *Xanthosoma sagittifolium* (L). In: Ofori F, Hahns SR (eds) Tropical root crops in a developing economy. Proc 9th Symp Int Soc for Tropical Root Crops. Accra, Ghana, pp 438–442

Andème-Onzighi C, Sivaguru M, Judy-March J, Baskin TI, Driouich A (2002) The *reb1-1* mutation of *Arabidopsis* alters the morphology of trichoblasts, the expression of arabinogalactan-proteins and the organization of cortical microtubules. Planta 215:949–958

Berg RH, Erdos GH, Gritzali M, Brown Jr RD (1988) Enzyme-gold affinity labelling of cellulose. J Electron Microsc Tech 8:371–379

Bluemenkrantz N, Absoe-Hansen G (1973) New method for quantitative determination of uronic acids. Anal Biochem 54:484–489

Bonfante-Fasolo P, Vian B, Perotto S, Faccio A, Knox JP (1990) Cellulose and pectin localisation in roots of *Mycorrhizal allium* porum: Labelling continuity between host cell wall and interfacial material. Planta 180:537–547

Boyer B, Nicole M, Potin M, Geiger JP (1997) Extracellular polysaccharides from *Xanthomonas axonopodis* pv. *Manihotis* interact with cassava cell wall during pathogenesis. Mol Plant Microb Inter 10:803–811

Brown I, Trethowan J, Kerry M, Mansfield J, Bolwell GP (1998) Localisation of components of the oxidative cross-linking of glycoproteins and callose synthesis in papillae formed during the interaction between non-pathogenic strains of *Xanthomonas campestris* and French bean mesophyll cells. Plant J 15:333–343

Cambion C, Vian B, Nicole M, Rouxel F (1998) A comparative study of carrot root tissue colonization and cell wall degradation by *P. violae* and *P. ultimum* two pathogens responsible for cavity spots. Can J Microbiol 44:221–230

Carnachan SM, Harris PJ (2000) polysaccharide compositions of primary cell walls of the palms *Phoenix canariensis* and *Rhopalostylis sapida*. Plant Physiol Biochem 38:699–708

Carpita NC, Gibeaut DM (1993) Structural models of primary cell walls in flowering plants: consistency of molecular structure with physical properties of the walls during growth. Plant J 3:1–30

Channarayappa J, Muniyappa V, Scwegler-Berry D, Shivashankar G (1991) Ultrastructural changes in tomato infected with tomato leaf curl virus, a white fly-transmitted geminivirus. Can J Bot 70:1747–1753

Chen WC, Hsieh HJ, Tseng TC (1998) Purification and characterisation of pectin lyase from *Pythium splendens* infected cucumber fruits. Bot Bull Acad Sci 39:181–186

Cherif M, Benhamou N, Belanger RR (1991) Ultrastructual and cytochemical studies of fungal development and host reactions in cucumber plants infected by *Pythium ultimum*. Physiol Mol Plant Pathol 39:353–375

Daayf F, Nicole M, Bélanger RR, Geiger JP (1997) Hyaline mutants from *Verticillium dalhiae*, an example of selection and characterisation of strains for host-parasite interaction studies. Plant Pathol 47:523–529

Delmer DP (1999) Cellulose biosynthesis, exciting times for a difficult field of study. Annu Rev Plant Physiol Mol Biol 50:245–276

Driouich A, Faye L, Staehelin A (1993) The Golgi apparatus is a factory for complex polysaccharides and glycoproteins. Trends Biochem Sci 18:210–214

Dube HC, Prabakaran K (1989) Cell wall degrading enzymes of *Pythium*. Plant Pathol 89:181–188

Gomez-Gomez L, Boller T (2002) Flagellin perception: a paradigm for innate immunity. Trends Plant Sci 7:251–256

Helbert W, Sugiyama J, Ishihara M, Yamanaka S (1997) Characterization of native cellulose in the cell walls of Oomycota. J Biotechnol 57:29–37

His I, Andème-Onzighi C, Morvan C, Driouich A (2001) Microscopic studies on mature flax fibers embedded in LR White: immunogold localization of cell wall matrix polysaccharides. J Histochem Cytochem 49:1525–1535

Hussey RS, Mims CW, Westcoot SW (1992) Immunocytochemical localisation of callose in root cortical parasitized by the ring nematode *Griconemella xenoplax*. Protoplasma 171:1–6

Isaac S (1992) Fungal plant confrontations. In: Isaac S (eds) Fungal - plant interactions. Chapman and Hall, London, UK, pp 147–207

Jacobs AK, Lipka V, Burton RA, Panstruga R, Strizhov N, Schulze-Lefert P, Fincher GB (2003) An Arabidopsis callose synthase, GSL5, is required for wound and papillary callose formation. Plant Cell 15:2503–2513

Knox JP, Linstead PJ, King J, Cooper C, Roberts K (1990) Pectin esterification is spatially regulated both within cell walls and between developing tissues of root apices. Planta 181:512–521

Mims CW, Sewall TC, Richardson EA (2000) Ultrastructure of the host-pathogen relationship in *Entomosporium* leaf spot disease of *Photonia*. Int J Plant Sci 161:291–295

Mueller WC, Morgham AT, Roberts EM (1994) Immunocytochemical localisation of callose in the vascular tissue of cotton plants infected with *Fusarium oxysporium*. Can J Bot 72:505–509

Murashige T, Skoog F (1962) A revised medium for rapid growth and bioassays with tobacco tissue cultures. Physiol Plant 15:473–497

Nishimura MT, Stein M, Hou BH, Vogel JP, Edwards H, Somerville SC (2003) Loss of a callose synthase results in salicylic acid-dependent disease resistance. Science 301:969–972

Omokolo ND, Tsala NG, Kanmegne G, Balange AP (1995) In vitro induction of multiple shoots, plant regeneration and tuberization from shoot tip of cocoyam. C R Acad Sci 318:773–778

Pacumbaba RP, Wutoh JG, Eyang SA, Tambong JT, Nyochembeng LM (1992) Isolation and pathogenicity of rhizosphere fungi of cocoyam in relation with cocoyam root rot disease. J Phythopathol 135:265–273

Ray B, Loutelier-Bourhis C, Lange C, Condamine E, Driouich A, Lerouge P (2004) Structural investigation of hemicellulosic polysaccharides from *Argania spinosa*: characterisation of a novel xyloglucan motif. Carbohydr Research 339:201–208

Schaffer JL (1999) Amélioration du système de culture du macabo (*Xanthosoma sagittifolium* L.Schott) en Pays bamiléké (Ouest-Cameroun). Cahiers Agricul 8:9–20

Schulze-Lefert P (2004) Knocking on the heaven's wall: pathogenesis of and resistance to biotrophic fungi at the cell wall. Curr Opin Plant Biol 7:377–83

Skutelsky E, Roth J (1986) Cationic colloidal gold - a new probe for the detection of anionic cell surface sites by electron microscopy. J Histochem Cytochem 34:693–696

Tambong JT, Poppe J, Höfte M (1999) Pathogenecity, electropheretic characterisation and in *planta* detection of cocoyam root rot disease pathogen *Pythium myriotylum* . Eur J Plant Pathol 105:597–607

Thiéry JP (1967) Mise en évidence des polysaccharides sur coupes fines en microscopie électronique. J Microsc 6:987–1018

Valette C, Nicole M, Sarah JL, Boisseau M, Boyer B, Fargette M, Geiger JP (1997) Ultrastructure and cytochemistry of interactions between banana and nematode *Rodopholus similis*. Fundam Appl Nematol 20:65–77

Valette C, Andary C, Geiger JP, Sarah JL, Nicole M (1998) Histochemical and cytochemical investigation of phenols in roots of banana infected by the burrowing nematode *Rodopholus similis*. Phytopathology 88:1141–1147

Vicré M, Jauneau A, Knox JP, Driouich A (1998) Immunolocalisation of β(1–6) and β(1–4) galactans in the cell wall and Golgi stacks of flax roots. Protoplasma 203:26–34

Viviane GAAV, van Dooijeweert W, Govers F, Kamoun S, Colon LT (2000) The hypersensitive response is associated with host and nonhost resistance to *Phytophthora infestans*. Planta 210:853–864

Vreeland V, Moise SR, Robichaux RH, Miller KL, Hua SST, Laetsch WM (1989) Pectate distribution and esterification in *Dubantia* leaves and soybean nodules, studied with a fluorescent hybridisation probe. Planta 177:435–446

Werner S, Steiner U, Becher R, Kortekamp A, Zyprian E, Deising HB (2002) Chitin synthesis during in planta growth and asexual propagation of the cellulosic oomycete and obligate biotrophic grapevine pathogen *Plasmopara viticola*. FEMS Microbiol Lett 208:169–173

Willats WGT, Limberg G, Buchholt HC, van Alebeek JG, Benen J, Christensen TMIE, Visser J, Voragen A, Mikkelsen JD, Knox JP (2000) Analysis of pectic epitope recognized by hybridoma and phage display monoclonal antibodies using defined oligosaccharides, polysaccharides, and enzymatic degradation. Carbohydr Res 308:149–152

Xu T, Omokolo ND, Tsala NG, Ngonkeu MLE (1995) Identification of the causal agent of cocoyam root rot disease in Cameroon. Act Mycol Sinica 14(1):37–45

Yeddidia I, Benhamou N, Chet I (1999) Induction of defence responses in cucumber plants (*Cucumis sativus* L.) by the biological agent *Trichoderma harzianum*. App Env Microbiol 65:1061–1070

Zamski E, Peretz I (1996) Cavity spot of carrots: cell wall degrading enzymes secreted by *Pythium* and pathogen-related proteins produced by the root cells. Ann Appl Biol 128:195–207

Zhang GF, Driouich A, Staehelin AL (1996) Monensin-induced redistribution of enzymes and products from Golgi stacks to swollen vesicles in plant cells. Eur J Cell Biol 71:332–340